

Target Recognition and Heavy Load Operation Posture Control of Humanoid Robot for Trolley Operation

Huiling Liu , Chengfang Luo and Lei Zhang

Abstract— This paper studies the method of target recognition and heavy load trolley control in humanoid robot pushing operation. In this paper, a piecewise fitting monocular vision ranging method is proposed to achieve the target search and location of humanoid robot NAO. Based on vision localization, the research of humanoid robot pushing operation is carried out, and the posture closed loop control of heavy load robot is carried out. The experimental results show the effectiveness and accuracy of the method of single eye distance measurement, target location and recognition and the control of the motion of the cart, and successfully completed the light load operation and heavy load operation of the humanoid robot dual-arm trolley.

I. INTRODUCTION

At present, many scientific researchers in many developed countries such as Japan and America have done a lot of work in the research and development of humanoid robot, and have made a breakthrough progress, humanoid robot has had a great impact on human life. Further, people hope that humanoid machines have the ability of "mobile operation" as human beings, that is, under the premise of steady walking with biped, the humanoid robot can realize reliable and efficient mobile task without changing the working environment, so that humanoid robot has potential strong application foreground, social benefit and economic benefit.

In the research of mobile operation of many robot carts, Georgia Institute of Technology based on the PR2 wheeled robot platform for Mobile target planning, control and sensing method, and its specific application, to promote the entire multi-functional vehicle, proposed a range of tracking and observation of the target controller, The results show that the robot has completed the

experiment stably and reliably in the typical office environment [1]. The Taiwan University of science and technology has put forward a method to locate the virtual target accurately. Through image segmentation, noise removal, image modification, image restoration and image representation, the virtual target is processed by image processing to make the location more accurate, and the transformation of the plane coordinates and the world coordinates is constructed by connecting four visual windows. Two visual navigation strategies [2],[3] based on virtual target location are analyzed. The University of Osaka, Japan, based on humanoid robot HRP-2 platform, takes into account the centroid COM, thrust and acceleration to realize force control [4],[5], solves the problem of the dynamic walking balance control of the humanoid robot in the driving task when there are external forces on the terminal actuator, considering the dynamic complementary zero moment Point (DCZMP), the dynamic stability balance of the humanoid robot is maintained in the process of single leg support and two foot support [6], and the validity of the method is proved by simulation and experiment. The University of Tokyo proposed a method of calculating the dual-arm reference force based on the estimation of frictional force, and proposed a thrust controller which can compensate the ZMP with the power feedback of the control hand, and the experimental results show that HRP-2 humanoid robot could drive 90kg wheelchair [7]. Beijing Institute of Technology based on BHR-2 humanoid robot platform, the maneuverability and task modeling of the dual-arm push handcart are analyzed. Through the simulation experiment, the task of the humanoid robot is realized successfully [8], and puts forward the compensation of wrist operation, and considers the expectation ZMP of stabilizing control in driving operation [9]. The University of Sherbrooke has proposed a humanoid robot to push the navigation of a shopping cart in a complex environment, using the whole body control to solve the effect of lateral swinging on the load, the results show that the experiment on humanoid robot Nao platform, without changing the hardware of humanoid robot, the effective load of humanoid robot increased significantly [10]. Then the

The authors are with the Beijing Key Laboratory of Robot Bionics and Function Research, Beijing Advanced Innovation Center for Intelligent Robots and Systems, Beijing University of Civil Engineering and Architecture, 10016 Beijing, China
leizhang@bucea.edu.cn

influence of vehicle and load on the stability of the robot is analyzed, and an effective solution is put forward to control the whole system [11].

Based on the humanoid robot NAO, this paper uses segmented fitting to locate the target and make cart steering and heavy load experiments. The humanoid robot searches the signs in the room by monocular vision to locate the target, and does the proximity and cart operation. The research contents include (1) the study of NAO robot monocular vision ranging method. A single eye distance measurement method using the target image pixel size for distance measurement is proposed. The model and implementation process of the method are described in detail, and the accuracy of the method is verified by the experiment. (2) the use of the NAO robot. The research on the method of target recognition and location by Naomark. (3) research on the method of NAO robot double arm pusher, including the research of steering and heavy load closed loop system.

II. A TARGET LOCATION METHOD BASED ON PIECEWISE FITTING

First, this paper presents a monocular Vision high precision range (within 2 meters) ranging method based on the pixel size of target imaging, this method uses the machine learning method to train the model, does not need to calibrate the camera, only needs to know the real size and the imaging size of the target, can calculate the distance between the target and the camera. Measurement accuracy can reach millimeter level. Finally, the target search and location are studied.

A. Method Principle and Data Acquisition

Naomark [12] is used as a range-finder in the experiment. The Naomark consists of a black circle and a white triangular fan. The fan sector revolves around the center of the circle and distinguishes the Naomark of different IDs by the specific positions of the different triangular sectors. The Naomark mainly contains Naomark shape information α , β , sizeX, sizeY and MarkId. wherein α is the Naomark and the camera horizontal angle of deflection, β is Naomark with the camera perpendicular angle, sizeX (sizeY) indicates the target Naomark image pixel size in the NAO robot vision, in radians (rad), MarkId represents the number of Naomark recognized, as shown in

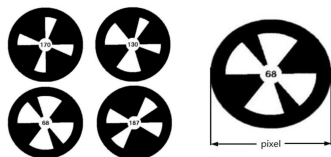


Figure 1. Naomark

Figure 1.

The NAO camera defaults to the 640*480 resolution, with a horizontal orientation of 640 pixels, and a vertical direction of 480 pixel points. The formula for sizeX is:

$$sizeX = \frac{pixel}{640} \times HOV \times \frac{\pi}{180} \quad (1)$$

where pixel represents Naomark imaging pixel diameter size, HOV represents the camera's horizontal angle of view, HOV=60.97°, the final calculated sizeX is in radians the number of units, SizeX represents the Naomark on the camera image size.

The experimental results show that the target has a certain relationship between the distance of the target and the camera with the relationship is found by the machine learning method, which is used to locate the NAO robot. Through experiments, the data of sizeX and distance between 0.2-2 m is recorded. As a result of camera photography, there is a certain distortion, distorted image pixel relative to the original image of the radial movement, and the farther away from the image center, the faster the speed of the external shift, that is, the image edge distortion than the image center distortion is greater. In order to reduce the error caused by distortion, the Naomark is first adjusted to the NAO robot's vision Center and then the pixel size of Naomark is read. A strategy of Nao robot to automatically adjust the Naomark to the center of vision is proposed below.

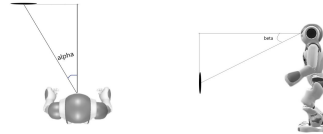


Figure 2. α and β

Adjust the Naomark to the center of the field of vision, first, the Naomark is identified and the angle relationship between the Naomark and the NAO robot is obtained. Then, reading the angle between the pitch axis (vertical direction) and the yaw axis (horizontal direction) of the NAO robot, β_0 , α_0 , and the angles between Nao robot and Naomark, β , α , as shown in Figure 2, get radian value from program. The angle of the head adjustment of Nao robot can be calculated by means of 2 and 3.

$$\alpha_1 = \alpha_0 + \alpha \quad (2)$$

$$\beta_1 = \beta_0 + \beta \quad (3)$$

where α_1 and β_1 are required to adjust the head angle. When α and β were considered to be lower

than 0.05 radians, Naomark was placed in the center of Vision. If not in the center of Vision, adjust the NAO head angle until the Naomark is placed in the center of Vision.

50 sets of data were obtained through experiments, in which the true size of the Naomark used was 10.9mm. Distance represents the real distance between the NAO robot camera and the Naomark, measured with a distance measuring instrument, measuring error 1mm, and the unit is M. The experiment recorded data from 0.195m to 1.846m, as shown in Figure 3. This set of data can be used to train the model of the single visual distance by machine learning method.

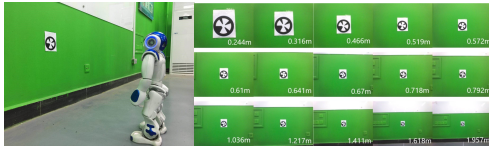


Figure 3. Monocular rangefinder

The 50 sets of data obtained from the experiment were drawn in the scatter chart to observe the changing trend of the data, as shown in Figure 4. The horizontal sizeX represents the target imaging size, and the longitudinal axis distance represents the distance between the camera and the target.

B. Fitting Method of Piecewise Distance Measuring Curve

The observation of Figure 4a shows that the distribution of scatter points between 0.2-2.0m tends to a smooth curve. Due to the effect of error, the distribution of scatter points between 1.0 M and 2.0m fluctuates slightly. This data is divided into two paragraphs to fit, that is, 0.2-1.0m for a paragraph, 1.0-2.0m for a paragraph, respectively, with a scatter picture, as shown in Figure 4b-c.

For 0.2-1.0m this segment, because the line between the scattered points is smoother, assuming that it tends to a polynomial curve, the polynomial fitting method is used to fit [13],[14],[15], and from

the fitting result, the error of calculating distance is the smallest when the scatter is proposed to synthesize 6 polynomial functions. Assume

$$f_M(x, w) = w_0 + w_1x + w_2x^2 + \dots + w_Mx^M \quad (4)$$

$$E(w) = \frac{1}{2} \sum_{i=0}^N \left(\sum_{j=0}^6 w_j x_i^j - y_i \right)^2 \quad (5)$$

Where x is sizeX, f represents Distance, and N represents the number of samples. Now we want to minimize the mean square error $E(w)$ and get the weight parameter w_j at this time. The partial derivative of w_j is zero.

$$\frac{1}{2} \sum_{i=2}^N 2 \left(\sum_{j=0}^M w_j x_i^j - y_i \right) \times x_i^k = 0 \quad (6)$$

$$\Rightarrow \sum_{i=0}^N \sum_{j=0}^M w_j x_i^j = \sum_{i=0}^N x_i^k y_i \quad (7)$$

Substituting 1-24 sets of data to obtain $(w_0, w_1, w_2, w_3, w_4, w_5, w_6) = (3.556, -51.111, 389.47, -1707.0, 4214.3, -5837.9, 3272.1)$. In the substitution type (4), we can get the expression after the scatter point is fitted, that is, through machine learning, we have learned the model of the relationship between sizeX and Distance within 1 meters.

$$f(x) = 3.556 - 51.111x + 389.47x^2 - 1707.0x^3 + 4214.3x^4 - 5837.9x^5 + 3272.1x^6 \quad (8)$$

For the 1.0-2.0m section, as shown in Figure 4c, the curve of the scattered point is not a smooth curve. In order to avoid the interference of the scatter point to the prediction model within 1 meters, the 1.0-2.0m section is fitted separately. Observe the scatter point of Fig 4c, and we can see a curve. For a humanoid robot double arm pusher, the requirement of robot visual distance

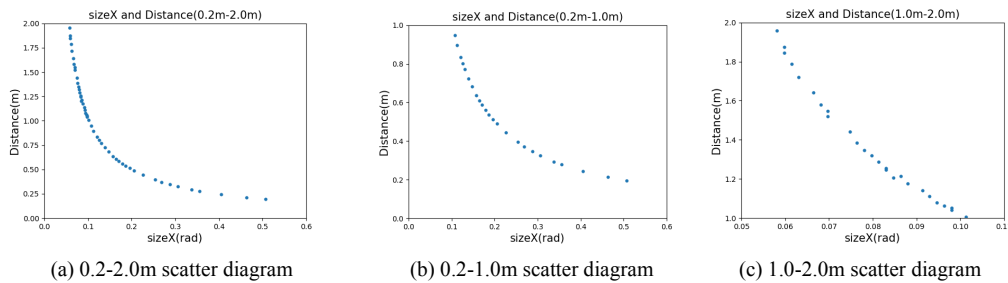


Figure 4. Image size and distance scatter plot

measurement is to measure the distance between the car and the car accurately when it is close to the car. It can be used to grasp the handle of the car accurately, while the robot can measure the distance accurately in the higher precision distance area when the robot is far away from the car, so the distance can be measured accurately in the high precision distance area. The precision of distance measurement is not high for one meter. For simplicity of calculation, the scatter point between 1-2m tends to a power function curve:

$$f(x) = bx^w \quad (9)$$

Make $f(x) \simeq y_i$. The pair (9) on both sides of the logarithm:

$$\lg f(x) = w \lg x + \lg b \quad (10)$$

The task of machine learning has become an attempt to learn (10), making $f(x) \simeq y_i$. Through logarithmic transformation, the problem of power function curve fitting is transformed to the simplest linear regression problem of [16],[17]. The mean square error (mean square error) is used to minimize the coefficients w and $\lg b$. Set mean square error:

$$E_{(w, \lg b)} = \arg \min_{(w, \lg b)} \sum_{i=1}^m (\lg y_i - w \lg x_i - \lg b)^2 \quad (11)$$

Get a partial derivative of w_j and make it 0

$$w = \frac{\sum_{i=1}^m \lg y_i (\lg x_i - \frac{1}{m} \sum_{i=1}^m \lg x_i)}{\sum_{i=1}^m \lg x_i^2 - \frac{1}{m} (\sum_{i=1}^m \lg x_i)^2} \quad (12)$$

TABLE I. EXPERIMENTAL RESULTS OF MONOCULAR RANGE FINDER

Experimental results within 1m					Experimental results between 1m-2m			
Numb er	sizeX (rad)	Distance(m)	Output (m)	Error(m)	Numb er	sizeX (rad)	Distance(m)	Output(m)
1	0.40357	0.244	0.24473	-0.00073	1	0.09965	1.036	1.01859
2	0.37036	0.268	0.26806	0.00001	2	0.09633	1.068	1.05971
3	0.31555	0.316	0.31461	0.00139	3	0.09134	1.126	1.12763
4	0.27071	0.368	0.36711	0.00089	4	0.08968	1.163	1.15205
5	0.23583	0.424	0.42314	0.00086	5	0.0847	1.217	1.23155
6	0.21424	0.466	0.46679	-0.00079	6	0.08138	1.277	1.29043
7	0.19265	0.519	0.51972	-0.00072	7	0.07972	1.332	1.32187
8	0.17604	0.572	0.56908	0.00292	8	0.07474	1.411	1.42531
9	0.16442	0.61	0.60964	0.00036	9	0.07307	1.484	1.46343
10	0.15611	0.641	0.64249	-0.00149	10	0.06975	1.555	1.54511
11	0.14947	0.67	0.67148	-0.00148	11	0.06643	1.618	1.63568
12	0.13951	0.718	0.72038	-0.00238	12	0.06477	1.677	1.68475

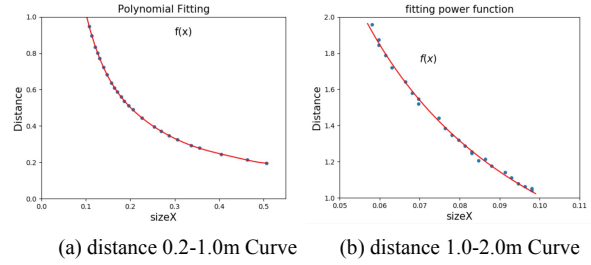


Figure 5. SizeX and distance diagram

$$\lg b = \frac{1}{m} \sum_{i=1}^m (\lg y_i - w \lg x_i) \quad (13)$$

By substituting 25-50 sets of data in the data set, we can get the model of monocular ranging based on $w = -1.168$, $b = 0.0689$ and substitution (9):

$$f(x) = 0.0689x^{-1.168} \quad (14)$$

The result of fitting is shown in Figure 5. In the distance 0.2m-1.0m, the six degree curve model is used to carry out the experiment. In the distance between 1.0m-2.0m, we use the trained power function curve model to carry out experiments. $f(x)$ is the output value of the model, representing the distance measured by the model, and x indicates the input value sizeX. It can be seen that the distance can be calculated as long as the image size sizeX of the target is input.

13	0.13286	0.757	0.75724	-0.00024	13	0.06311	1.743	1.73662
14	0.12788	0.792	0.7874	0.0046	14	0.06145	1.81	1.79154
15	0.12124	0.836	0.83142	0.00458	15	0.05979	1.875	1.84977
16	0.11626	0.871	0.86763	0.00337	16	0.05813	1.957	1.91161
17	0.11293	0.895	0.89352	0.00148				
18	0.10961	0.924	0.92077	0.00323				
19	0.10795	0.947	0.93497	0.01203				
20	0.10297	0.998	0.97996	0.01804				

The experimental results, as shown in Table 1, show that the measurement error within 0.947m is in the millimeter level, the maximum error is 4.6mm and the average error is 1.7mm. The error is mainly from the instrument measuring the real distance and the error of the measuring instrument is 1mm; the error after 0.947m is gradually increased to the level of millimeter. The average measurement error between 1m-2m is 1.51cm, the maximum error is 4.5cm at 1.957m, and the minimum error is 1.6mm at 1.23m. It can be seen that the single eye range finding algorithm within 1m can achieve high accuracy, the average error within 1m is only 1.7mm, and the error in the 1m-2m interval measurement is slightly larger, but the average error is only 1.51cm. This error is in line with the NAO robot positioning small car and accurately catching the request of the handle of the car.

III. TARGET SEARCH AND LOCATION OF HUMANOID ROBOT

Target search and location is a key part in the research of humanoid robot double arm trolley operation. In the living environment of human-machine coexistence, the humanoid robot must complete the task of searching and identifying the trolley and the positioning car independently.

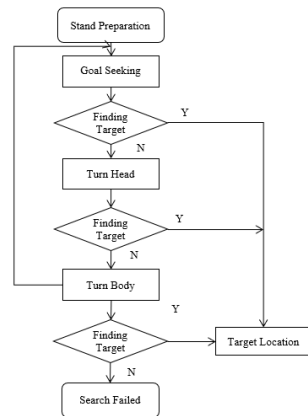


Figure 6. Nao robot search target flow chart

The humanoid robot determines whether it is a trolley by obtaining the ID number of the Naomark. First, the Nao robot is prepared for standing,

waiting for the target search instruction. After receiving the target search instruction, it first searches for the target in the current field of vision. Without the target, it changes the angle of the head joint. If there is a target, the target begins to be adjusted to the center of the vision to facilitate the measurement. When the target is found, the joint angle is changed and the head angle search is continued until the target is found. Because the NAO robot software system is integrated with the program to identify the Naomark, the direct call to the Memory of the NAO robot can obtain the identified information. Therefore, the Naomark is attached to the small cart in the experiment, and the NAO robot is used to identify the Naomark, and the NAO robot can be searched for the car. The search process flow chart is shown in Figure 6.

The location of trolley uses monocular vision ranging. Judge whether the distance is in the range of precise distance measurement, then move the car close to the car accurately. After reaching the target, grab the trolley handle and prepare the cart. This method does not need to calibrate the camera, reducing the workload caused by calibrating the camera.

When Naomark appears in the NAO robot's field of vision, adjust the orientation of the NAO robot, so that the target is aligned with the robot. Then start the distance algorithm to calculate the distance between the robot and the Naomark. When the distance between the car and the car is far away, the laissez faire robot NAO walks close to the car, in which $x = \text{Distance} - 0.7$, the purpose is to make the NAO robot enter the range of the range of higher accuracy of the single eye distance measurement, When the NAO robot enters a precise and high range, it can perform precise ranging and determine whether the NAO robot is on the car handle, if not facing the handle of the car, can adjust the transverse distance and position of the humanoid robot NAO to the handle of the car, and y is the number of crosswise.

Distance is the distance between the NAO camera and the Naomark calculated by the monocular range finding algorithm, the Y is the transverse distance between the NAO robot and the Naomark, and the X is the longitudinal distance

between the NAO robot and the Naomark. The values of X and y can be calculated by the trigonometric function relation:

$$y = \text{Distance} \times \sin(\alpha_0) \quad (15)$$

$$x = \text{Distance} \times \cos(\alpha_0) \quad (16)$$

NAO robot search and locate the car's experiment is shown in Figure 7.

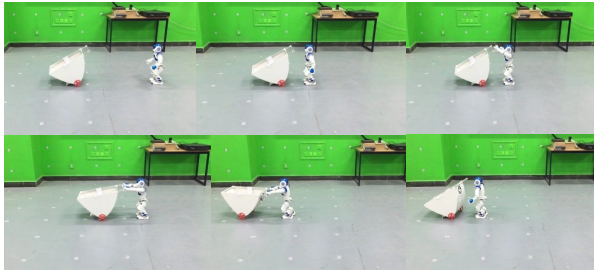


Figure 7. NAO light load cart experiment

IV. POSTURE CONTROL OF DUAL-ARM

According to the monocular vision ranging method introduced in the second section and target search and location, the task of humanoid robot double arm trolley operation is carried out. After the search is successful and the target is located, the double arm cart task is started. The experiment is carried out under light load and heavy load.

A. Light load Experiment

The light load car is a two wheeled structure. The area with a wide field of vision under the handle of the car is affixed with Naomark for NAO identification and location. The vehicle weight is 1.5kg. When the NAO robot searches for the car, it arrived the car and then close to the handle of the car. When it reaches 0.18m from the car, it begins to carry the handle of the car and begins to push the cart, as shown in Figure 7. In the experiment, NAO measured the distance between the car and the car by 0.925m, and the distance from the cart was 1 meters. Push the cart to the destination and put the cart back and reset it.

The humanoid robot's two arms are sufficient to restrict and control all the degrees of freedom of the trolley. The research shows that Honda's ASIMO can move a trolley to freely in rooms and corridors. However, the robot mainly controls a Dubins vehicle rather than taking full advantage of the full motion of the humanoid robot. In addition, the arm is only used as a means of attaching the vehicle to the robot, and no further consideration is given to the control vehicle. Another study used bipedal robot wheelchair. In order to maintain balance when performing the required tasks, this HRP-2 and ASIMO have implemented a zero moment

point (ZMP) migration method. Although HRP-2 has a heavy load of mobile wheelchairs, it is similar to ASIMO robots that control cars like Dubins. In addition, none of these examples minimizes the footprint of the robot trolley device by rotating objects, because they are regarded as a static set. In a compact and cluttered environment, manipulating objects like trolley with arms is beneficial and necessary.

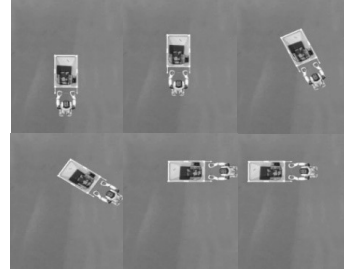


Figure 8. Nao cart steering

The NAO robot's steering method in light load trolley is shown in Figure 8. Because the car is a two-wheeled structure and the two wheels are rotated independently, the car can rotate around the middle point between the two wheels of a small car. Using this rule, when the NAO robot pulley needs to be turned, the NAO robot is added along the lateral circular arc trajectory. The track of the motion is the center of the middle point of the two wheels of the car and the NA. The distance from the O robot to the midpoint of the two wheels is the arc of the radius. When the cart is required to turn left, the NAO robot moves counterclockwise along the circular track; when the cart needs to be turned right.

B. Heavy Load Control Experiment

The NAO robot will be disturbed by the counterforce of the trolley. When the load is large enough, the NAO robot can't balance the reaction



Figure 9. Heavy load cart

force of the car on the dual arm of the NAO robot. This will break the equilibrium state of the NAO robot and make the robot lose its balance and fall. The research on pushing heavy objects by humanoid robot is a hot topic in the field of biped robots, and its research is very difficult. Humanoid robots are largely balanced by their feet, so it is difficult to maintain a balance when they are disturbed by large disturbances. So far, humanoid robots have not been able to resist external

disturbances as strong as human beings. If human beings can drive tens of times the weight of their weight on a horizontal road, humanoid robots are still unable to drive tens of times the weight of their weight. The main reason is that the balance of humanoid robots is difficult to control, and of course, the effects of joint driving force.

In order to study the situation of the humanoid robot's heavy load vehicle, a car specially capable of carrying the maximum weight is specially produced, as shown in Figure 9. The vehicle has four universal wheels, which can theoretically bear the load capacity of 100kg. It can meet the experimental requirements of NAO robot's heavy load vehicle. In the experiment, let the NAO robot push the 29.3kg car. The quality of the tigers is 15kg, the quality of the toolbox is 5.5kg, the quality of the drawer is 4.6kg, the mass of the cart is 4.2kg, the total mass is 29.3kg, the NAO robot is 4.5kg, and the total quality of the truck is about 6.5 times the quality of the NAO robot.

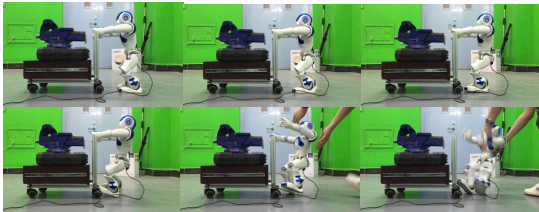


Figure 10. Nao robot loss balance

The model of a humanoid robot NAO is controlled, in Figure 10. As shown in Figure 9, it can be seen from the diagram that the NAO robot is still stride forward when it is unable to push the car, causing the body to move back. At this time, the NAO robot trolley system is an open loop control system, and the NAO robot can't receive feedback from the cart. Signal. The result is that the NAO robot can't drive heavy vehicles, eventually losing balance and falling down.

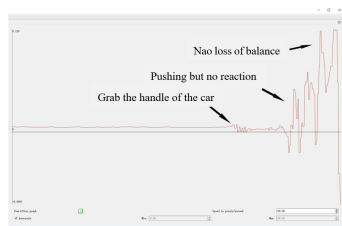


Figure 11. Robot gyroscope waveform diagram

The continuous curve in Figure 11 shows the movement of the X axis in the NAO gyroscope, which represents the tilt of the NAO robot body in front and rear directions.

To make the NAO robot able to drive a car weighing 6.5 times its own weight, here is a method of NAO robot pushing the car. A closed loop system is built according to the output of the X axis of the gyroscope, as shown in Figure 12.

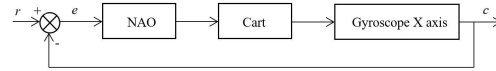


Figure 12. Closed loop system of NAO trolley



Figure 13. NAO push heavy load car

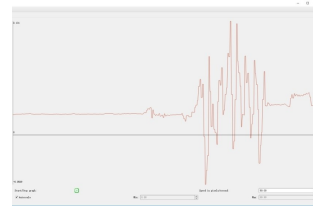


Figure 14. NAO push heavy load trolley gyroscope waveform

In this system, r represents the control input generated by adjusting the angle of the torso, and c represents the output of the X axis of the NAO gyro. From Figure 10, we can see that when the system is balanced, the output of the closed loop system is $c=0.007$, when $c=0.129$ will completely break the stability of the system and can't be automatically adjusted to restore stability. In this system, the input r of the system is generated by adjusting the trunk angle. This function can set up the left and right hip joint LHipPitch and RHipPitch of the NAO robot. By adjusting the input amount R , the disturbance caused by the NAO heavy truck is offset by negative feedback. After a closed loop system is designed to control the NAO trolley, the NAO can drive a car with 6.5 times heavier than itself. The cart process is shown in Figure 13, and the state of the gyroscope's X axis is shown in Figure 14.

The experimental results show that after adding the closed loop system, the humanoid robot NAO successfully promotes the target object of 6.5 times its own weight.

V. CONCLUSION

This paper first introduces the hardware and software system of a small humanoid robot NAO,

including its basic information such as joint and structure, visual system, sensor, software environment, development language and so on. Secondly, a high accuracy distance measurement method based on machine learning for monocular vision is introduced. Then the research on the humanoid robot's pushing operation is carried out, including the study of the cart turning and the study of the heavy load vehicle. Finally, the contents of the experiment are verified. In the experiment, the small humanoid robot NAO is able to locate the car accurately and grasp the handle of the car by using the single visual range, which can locate the car accurately and grasp the handle of the car. At the same time, the NAO robot has completed the automatic push cart operation, the cart steering and the heavy load trolley operation. The light vehicle experiment is based on monocular vision ranging, which further verifies the feasibility of monocular vision ranging in humanoid robot double arm cart operation. In the experiment of a heavy truck, a heavy load car with a weight of 6.5 times heavier than its weight is demonstrated by NAO. The feasibility of a closed loop control system based on the X axis of the body gyroscope is verified. Of course, there are many shortcomings in our method, and there are many areas to be improved, in which the amount of data in the distance measurement is not enough, and the experimental data is not accurate enough, and the method in the experiment of the cart needs to be improved. Finally, it is proved by experiments that the methods of monocular vision ranging, target search and location, and cart operation are efficient and reliable, and the research on the experiment system of humanoid robot double arm pusher is completed.

ACKNOWLEDGMENT

Supported by the National Natural Science Foundation of China (Grant No. 61473027), and Beijing Key Laboratory of Robot Bionics and Function Research (Grant No. BZ0337), and Supported by The Fundamental Research Funds for Beijing Universities, and Beijing Advanced Innovation Center for Intelligent Robots and Systems, and Beijing Advanced Innovation Center for Future Visual Entertainment.

REFERENCES

- [1] Jonathan Scholz, Sachin Chitta, Bhaskara Marthi, and Maxim Likhachev. Cart pushing with a mobile manipulation system: Towards navigation with moveable objects. In IEEE International Conference on Robotics and Automation, 2011:615-620.
- [2] Chih-Lyang Hwang, Ying-Jer Chou, and Chien-Wu Lan. Comparisons between two visual navigation strategies for kicking to virtual target point of humanoid robots. IEEE Transactions on Instrumentation & Measurement, 2013, 62 (11) :3050-3063.
- [3] Chih-Lyang Hwang, Ying-Jer Chou, and Chien-Wu Lan. "Search, Track, and Kick to Virtual Target Point" of humanoid robots by a neural-network-based active embedded vision system. IEEE Systems Journal, 2015,9 (1) :107-118.
- [4] Kotaro Sakata, Kenji Inoue, Tomohito Takubo, Tatsuo Arai and Yasushi Mae. Wheelchair user support system using humanoid robots: system concept and experiments on pushing wheelchair. Sice Conference.2004,2(2):1650-1655.
- [5] Tomohito Takubo, Kenji Inoue and Tatsuo Arai. Pushing Operation for Humanoid Robot Using Multipoint Contact States. IEEE/RSJ International Conference on Intelligent Robots and Systems, 2005,79 (4) :1887-1892.
- [6] Tomohito Takubo, Kenji Inoue and Tatsuo Arai. Pushing an Object Considering the Hand Reflect Forces by Humanoid Robot in Dynamic Walking. IEEE International Conference on Robotics and Automation, 2006 :1706-1711.
- [7] Shunichi Nozawa, Yohei Kakiuchi, Kei Okada and Masayuki Inaba. Controlling the Planar Motion of a Heavy Object by Pushing with a Humanoid Robot using Dual-arm Force Control. IEEE International Conference on Robotics and Automation, 2012,44 (8) :1428-1435.
- [8] Tao Xiao, Min Li, Qiang Huang, Weimin Zhang, and Le He. Analysis of Pushing Manipulation by Humanoid Robot BHR-2 during Dynamic Walking. IEEE International Conference on Automation and Logistics, 2007:3000-3005.
- [9] Tao Xiao, Qiang Huang, Junyao Gao, and Weimin Zhang. Manipulability and Stability of Pushing Operation by Humanoid Robot BHR-2. IEEE International Conference on Robotics and Biomimetics, 2008 :751-756.
- [10] Antoine Rioux and Wael Suleiman. Humanoid Navigation and Heavy Load Transportation in a Cluttered Environment. IEEE/RSJ International Conference on Intelligent Robots and Systems, 2015 :2180-2186.
- [11] Louis Hawley and Wael Suleiman. Control Strategy and Implementation for a Humanoid Robot Pushing a Heavy Load on a Rolling Cart. IEEE/RSJ International Conference on Intelligent Robots and Systems, 2018 :4997-5002.
- [12] <http://doc.aldebaran.com/2-1/naoqi/vision/allandmarkdetection.html>
- [13] Bin Jiang and Hua Guo. Permutation invariant polynomial neural network approach to fitting potential energy surfaces. Journal of Chemical Physics, 2013,139 (5) :204103.
- [14] Alvise Sommariva and Marco Vianello. Polynomial fitting and interpolation on circular sections. Applied Mathematics & Computation, 2015,258 :410-424.
- [15] Fumiki Sekiya and Akihiro Sugimoto. Fitting discrete polynomial curve and surface to noisy data. Annals of Mathematics and Artificial Intelligence, 2015,75 (1-2) :135-162.
- [16] Eric Pqi and Fred Yye. Data Fitting and Theoretical Analysis of the Shifted Power Function. Journal of the China Society for Scientific and Technical Information, 2016,12.
- [17] Qiu Tian, Hua Wei ping and Li Xinguang. Hypothesis Testing for Parameters in Normal Linear Regression Model Under Dual Power Transformation. Statistics & Decision, 2017,02.